Oceanographic investigation of the American Samoa albacore (*Thunnus alalunga*) habitat and longline fishing grounds

RÉKA DOMOKOS,[1,*] MICHAEL P. SEKI,[1] JEFFREY J. POLOVINA[1] AND DONALD R. HAWN[2]

[1]*National Marine Fisheries Service, NOAA, Pacific Islands Fisheries Science Center, 2570 Dole Street, Honolulu, HI 96822-2396, USA*
[2]*Joint Institute for Marine and Atmospheric Research, University of Hawaii, 1000 Pope Road, Honolulu, HI 96822, USA*

ABSTRACT

The American Samoa fishing ground is a dynamic region with strong mesoscale eddy activity and temporal variability on scales of <1 week. Seasonal and interannual variability in eddy activity, induced by baroclinic instability that is fueled by horizontal shear between the eastward-flowing South Equatorial Counter Current (SECC) and the westward-flowing South Equatorial Current (SEC), seems to play an important role in the performance of the longline fishery for albacore. Mesoscale eddy variability in the American Samoa Exclusive Economic Zone (EEZ) peaks from March to April, when the kinetic energy of the SECC is at its strongest. Longline albacore catch tends to be highest at the eddy edges, while albacore catch per effort (CPUE) shows intra-annual variability with high CPUE that lags the periods of peak eddy activity by about 2 months. When CPUE is highest, the values are distributed toward the northern half of the EEZ, the region affected most by the SECC. Further indication of the possible importance of the SECC for longline performance is the significant drop in eddy variability in 2004 when compared with that observed in 2003 – resulting from a weak SECC – which was accompanied by a substantial drop in albacore CPUE rates and a lack of northward intensification of CPUE. From an ecosystem perspective, evidence to support higher micronekton biomass in the upper 200 m at eddy boundaries is inconclusive. Albacore's vertical distribution seems to be governed by the presence of prey. Albacore spend most of their time between 150 and 250 m, away from the deep daytime and shallow nighttime sonic scattering layers, at depths coinciding with those of small local maxima in micronekton biomass whose backscattering properties are consistent with those of albacore's preferred prey. Settling depths of longline sets during periods of decreased eddy activity correspond to those most occupied by albacore, possibly contributing to the lower CPUE by reducing catchability through rendering bait less attractive to albacore in the presence of prey.

Key words: albacore tuna, American Samoa EEZ, longline fishery, mesoscale eddy, micronekton distribution, mid-ocean eddies, sonic scattering layer (SSL), South Equatorial Counter Current (SECC)

INTRODUCTION

The American Samoa domestic longline fishery began operating in the central South Pacific waters in 1995, targeting primarily albacore tuna, *Thunnus alalunga*. During the first 4 years, most longline fishing around American Samoa was accomplished through a fleet of smaller, approximately 10 m in length, open-decked catamarans known as 'alia'. However, during 1999–2001, the fishery experienced extraordinary growth – particularly in the fleet composition of large vessels (>20 m in length) – that fueled a fivefold increase in fishing effort and landings. For example, only 23 vessels made up the fishery in 1999, deploying 2102 sets (approximately 0.91 million hooks), resulting in catch rates of about 32 fish per 1000 hooks. In comparison, more than 50 boats actively participated in the fishery during 2001, deploying 4690 sets (more than 5 million hooks), yielding about 40 fish per 1000 hooks. This increase in both the number of sets and hooks per set was not only a result of the increase in the number of fishing vessels but also of the increase in the size of the vessels and their ability to travel farther from port.

Very few studies have been published with regard to the pelagic habitat and the spatial and temporal variability of the oceanographic climate in the American Samoa region. Historical studies conducted on South Pacific longline fisheries and the corresponding

*Correspondence. e-mail: reka.domokos@noaa.gov
Received 23 August 2006
Revised version accepted 2 March 2007

 doi:10.1111/j.1365-2419.2007.00451.x

environment have focused on foreign fishing activities primarily in waters farther to the west, e.g., west of Fiji (Yamanaka, 1956; Saito, 1973). More recently, a comprehensive simultaneous investigation of tuna, its forage, and the environment was carried out within the framework of the Etude du Comportement des Thonidés par l'Acoustique et la Péche (ECOTAP; Study of Tuna Behavior using Acoustics and Fishing) in the French Polynesian Exclusive Economic Zone (EEZ), located east of the American Samoa EEZ (e.g. Josse *et al.*, 1998; Bertrand *et al.*, 1999, 2002a,b). Large-scale oceanographic circulation patterns suggest that the waters of both French Polynesian and American Samoa EEZ are heavily influenced by the meandering flow of the South Equatorial Current (SEC) (Lukas, 2001). However, the American Samoa EEZ (Fig. 1) lies in the path of the seasonally varying South Equatorial Counter Current (SECC), which mostly dissipates before reaching the French Polynesian EEZ. The SECC flows eastward from about 7–8°S to 12–13°S and over the northern section of the EEZ, peaking in amplitude from March to April (Qiu and Chen, 2004). Strong horizontal shear between the westward-flowing SEC and the eastward-flowing SECC results in barotropic instability followed by seasonally modulating mesoscale eddy kinetic energy levels.

The presence of mesoscale eddies – as well as their detection by the fishery fleet – has been shown to be an important factor in fishery performance, leading to increased catch per effort for albacore tuna (e.g. Laurs and Lynn, 1977; Laurs *et al.*, 1984). Horizontal shear at eddies and fronts is known to concentrate large animals such as tuna, presumably to feed on the larger aggregations of food resources such as micronekton (e.g. Murphy and Shomura, 1972; Fiedler and Bernard, 1987). Changing physical conditions within cyclonic and anticyclonic eddies can also result in preferential aggregation or avoidance of the eddy cores by certain

Figure 1. Map of the American Samoa Exclusive Economic Zone (EEZ) with mean satellite sea surface heights for the week of March 7–13, 2004. Tutuila, the largest island of American Samoa, is located at 170°45′W, 14°15′S with the next largest islands at 169°30′W, 14°10′S. Black line: boundary of the EEZ; magenta line: cruise tracks of the *Oscar Elton Sette*, March 3–15, 2004; red line: boundary of albacore and longline tagging operations (Box 1), February 29 through March 16, 2004. Arrows indicate the calculated geostrophic currents.

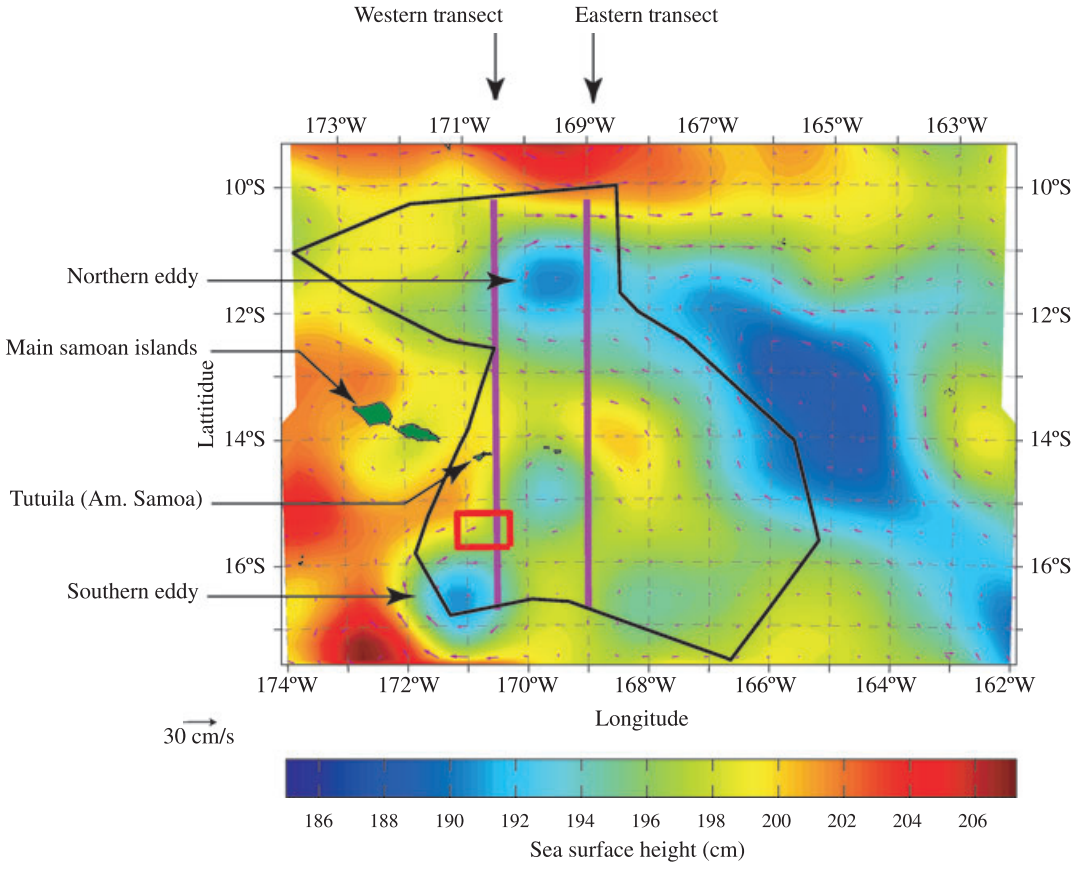

organisms, such as various target species of commercial fisheries and their primary prey, mesopelagic micronekton. For example, cyclonic eddies can impact local phytoplankton production as a result of the enhanced upwelling of nutrients (e.g. McGillicuddy *et al.*, 1998; Oschlies and Garcon, 1998; Seki *et al.*, 2001), which in turn can increase micro- and mesozooplankton production in these regions (e.g. Wiebe *et al.*, 1985; Piontkovski *et al.*, 1995; Zimmerman and Briggs, 1999). However, few studies have addressed the effects of mesoscale eddies on micronekton communities, which are the main food source for some larger predatory nekton such as tuna. Furthermore, all of our knowledge on the effects of eddies on the distribution of micronekton is based on studies that focus on frontal eddies associated with energetic boundary currents (e.g. Brandt, 1981; The Ring Group, 1981; Wiebe and Joyce, 1992; Sassa *et al.*, 2002), or on eddies formed by the interaction of boundary currents with topography (Ménard *et al.*, 2005). As opposed to these latter eddies, the eddies associated with the boundary region of the SEC and SECC are formed by barotropic instability and – as the SECC originates from the SEC to the east of New Guinea – are expected to form within a relatively homogeneous water mass. Characteristic differences between boundary current and mid-ocean eddies are expected to result in distinct effects on the local micronekton communities at the two types of eddies either by advecting the communities into the area or by locally enhancing their development.

Albacore tuna, *Thunnus alalunga*, is the target species in the American Samoa fishery and dominates the catch (WPRFMC, 2001; DMWR, 2002). Longline fisheries, such as those operating in Samoan waters, specifically target and harvest the deeper dwelling, larger-sized mature albacore that, like bigeye tuna, *Thunnus obesus*, have catch rates that increase in proportion to depth fished (Boggs, 1992; Nakano *et al.*, 1997). Local surface troll fishers also target species considered to occupy shallower depths, including blue marlin (*Makaira nigricans*), wahoo (*Acanthocybium solandri*), mahimahi (*Coryphaena hippurus*), and skipjack tuna (*Katsuwonus pelamis*). Concerns now abound that the rapidly expanding fleet is affecting the local supply of these large pelagic fishery resources. Observed negative trends in both the longline and troll catch rates of the shallow species do little to suppress these fears. To address these concerns, a 50-nautical-mile fishing area closed to the large vessels was designated in 2002 around the American Samoa islands and a limited entry program has been implemented on the region's fishery (Federal Register; Anonymous, 2002).

Another concern for the fishers is their ability to set their longline gear into the depths occupied by mature albacore. Depth distribution of albacore in the Pacific ranges from the surface to at least 380 m and is typically governed by the vertical thermal structure and oxygen concentration of the water column (Collette and Nauen, 1983). Saito (1973) reported that large-sized albacore are broadly found at depths ranging from 80 to 380 m, but the center of their vertical distribution is about 200 to 260 m below surface. Interestingly, much of the incidental catch in the domestic American Samoa deep longline fishery is composed of the shallow-dwelling fauna, such as those described above. Horizontal shear associated with strong currents – such as the SEC and SECC – could reduce the likelihood of getting longline gear to settle in the desired deeper waters for albacore (e.g. Mizuno *et al.*, 1994; Bigelow *et al.*, 2006); final longline set depths have been reported to be considerably shallower (e.g. 54–68%) than target depths Boggs (1992). It is possible that the American Samoa fishery longline sets likewise settle at shallower depths than intended, making the shallower dwelling species more available to the gear.

The objectives of this study were to determine the physical and biological characteristics of the American Samoa pelagic habitat and fishing grounds; that is, (1) understand the spatial and temporal occupation patterns and movements of large South Pacific albacore, and (2) to examine the role that the environment might have on albacore distribution as well as on longline gear performance and catch. Identifying oceanographic features of tuna habitat and understanding characteristics that affect the spatial and temporal distribution of albacore will help in developing and maintaining sustainable fishing practices for this commercially important species.

METHODS

Based on the interdisciplinary nature of this work, a multiplatform approach involving data from a variety of sources was implemented. The oceanographic characteristics of the pelagic habitat fished by the American Samoa longline fishery, and particularly, that of the EEZ, were assessed using *in situ* shipboard conductivity–temperature–depth (CTD) surveys together with satellite altimetry data. Information on the performance of the American Samoa commercial longline fishery was collected using catch data for albacore from the American Samoa fishery shipboard logs, while longline depths were inferred from temperature and depth recorders attached to commercial longline sets. Depth distribution of albacore within

the American Samoa fishing grounds was monitored via pop-up archival tags. Furthermore, relative density of micronekton within the fishing grounds was estimated via *in situ* shipboard acoustic measurements.

Oceanographic characteristics of the fishing grounds

In situ hydrographic data were collected with CTD casts aboard the NOAA ship *Oscar Elton Sette* between March 3 and March 13, 2004. Casts to 1000 m were conducted along two meridional transects located on 170°30′W (the 'western transect') and on 169°00′W (the 'eastern transect') from 10°15′S to 16°45′S, spaced 15 nautical miles (1 nmi ≃ 1852 m) apart from each other (Fig. 1). All casts used a SeaBird SBE 9/11+ CTD system equipped with redundant temperature, conductivity, and dissolved oxygen sensors (Seabird Electronics, Inc., Bellevue, WA, USA) and a Seapoint fluorometer (Seapoint Sensors, Inc., Exeter, NH, USA) for *in vivo* chloropigment (chlorophyll + phaeopigments) determinations.

Sea surface heights (SSH) were obtained from the Ssalto program of the Centre National d'études Spatiales, France, for the years 1996–2004 for the area of 172°W to 148°W, 30°S to 5°N, to correspond in time to the American Samoa longline fishery logbooks (see below) and in space to the fishing grounds (e.g. Fig. 1). The SSH data obtained were the AVISO TOPEX/POSEIDON altimetry product from January 1996 to July 2002, after which JASON-1 was put into operation replacing TOPEX/POSEIDON and providing altimetry along the same orbit with similar resolution. The AVISO TOPEX/POSEIDON–JASON-1 altimetry product contains the weekly averages of sea-level anomalies of along-track profiles mapped to a global 0.3° × 0.3° mercator projection. The SSH anomalies were calculated as relative to the mean of the SSH along-track TOPEX/POSEIDON profiles from 1993 to 1998. These weekly 0.3° × 0.3° SSH anomalies from Ssalto were then added to the 1994 NODC World Ocean Atlas Levitus long-term mean dynamic heights and gridded to create a 0.25° × 0.25° 'absolute' SSH field over the study area. Geostrophic current components were calculated from the 'absolute' TOPEX/POSEIDON–JASON-1 SSH using the hydrostatic approximation with the reference level assumed to be at 1000 m below surface (e.g. Gill, 1982), while gradients were taken using the forward–backward scheme resulting in a 0.5° × 0.5° resolution current field.

American Samoa longline fishery performance and albacore depth distribution

The American Samoa commercial longline fishery logbook program was implemented in 1996 to monitor the fishery activities. For this study, these logbook records were used to obtain information on the number of hooks and number of albacore caught by longline gear – along with time and location information of longline sets – for the years 1996–2004. Settling depths of longline gears were examined using temperature and depth recorders (TDRs) that were attached to three sets deployed within an area defined by 170°17.1′W to 171°1.8′W and 15°15.4′S to 15°32.9′S, herein referred to as 'Box 1' (Fig. 1), on February 29, March 1, and March 2, 2004. Each of the three sets were equipped with six LOTEK Fish & Wildlife Monitoring Systems LTD_1100 archival tags (Lotek Wireless, Inc., Newmarket, Canada) spaced along a single section of longline (defined by a pair of consecutive floats), each recording data at approximately 3.75-min intervals.

To study albacore tuna depth distribution in the American Samoa region, six tuna were equipped with Wildlife Computers Pop-up archival transmitting (PAT) tags between February 29 and March 2, 2004, within Box 1 (Fig. 1). Fork lengths for the six albacore were between 93 and 105 cm, corresponding to young adult fish and representative of mean longline catch in the EEZ. In an effort to balance the limited battery life (and the maximum number of 'live days') with the increase in temporal resolution, three of the tags were programmed to collect depth and temperature data in 1-h bins, while the other three, to conserve battery power and increase the life of the tags, were programmed to collect data in 4-h bins. Binned records were uploaded to the ARGOS satellite once the tags detached from the fish and floated to the surface. The temperature and depth records downloaded from the satellite were further grouped into 50-m depth bins starting with 0–50 m down to 950–1000 m, with an additional bin containing all data obtained below 1000 m depth.

Micronekton distribution

To examine the horizontal and vertical patterns of micronekton distribution and abundance in the American Samoa fishing grounds, relative micronekton densities were estimated using *in situ* acoustic backscatter data collected on board the NOAA ship *Oscar Elton Sette* between March 3 and March 15, 2004. The acoustic transects correspond to the two meridional transect lines discussed in the preceding section (Fig. 1). The acoustic scattering data were collected using a Simrad EK60 split beam echosounder system operating at 38- and 120-kHz frequencies (Simrad, Horten, Norway). The dual frequency system was used to obtain information on the relative com-

position of the sonic scattering layer (SSL), as organisms have distinct scattering properties at the two frequencies. Both transducers had approximately 7° beam widths and were set to operate with pulse lengths 512 and 256 μs for the 38- and 120-kHz frequencies, both at 1-kW power. These settings gave ranges of 800 and 200 m for the two frequencies, with a nominal depth-dependent threshold for a signal-to-noise ratio of 10 dB for the mean volume backscattering strengths, S_v (MacLennan and Simmonds, 1992). The highest threshold at the deepest ranges was −70 dB for both frequencies. Before processing the data, each echogram was visually inspected and all areas contaminated by noise were removed. For the purposes of estimating relative biomass, S_v were integrated over 50-m long by 5-m deep bins, using SonarData Echoview® software (SonarData Pty Ltd, Hobart, Australia), and the resulting mean nautical area scattering coefficients (NASC $\equiv s_A$), in units of m^2 nmi^{-2} (MacLennan *et al.*, 2002), were exported for further processing. The resulting NASC were used as a proxy for relative biomass estimates, as they are proportional to biomass, assuming that the species composition of the scattering layer and the resulting scattering properties of the micronekton do not change significantly (MacLennan and Simmonds, 1992).

As the SSL is composed mostly of organisms undergoing diel vertical migration, daytime and nighttime NASC had to be analyzed separately. Thus, both the 38- and 120-kHz bioacoustic records were divided into daytime and nighttime components to be examined separately. Two 3-h windows, one from 05:00 to 08:00 hours and another from 17:00 to 20:00 hours, were deemed sufficient to remove effects from all transition periods. Data from only the upper 500 and 200 m were included in the analysis for the 38- and 120-kHz channels because of unacceptably low signal-to-noise ratios below those depths – a result of bad weather – during much of the recordings. As a result of excluding data from below these depths, only the shallow scattering layer could be analyzed.

RESULTS

Physical properties

Weekly SSH averages from satellite altimetry revealed the presence of eddies and meanders in the American Samoa fishing grounds and temporal variability with scales less than a week. For example, the cyclonic eddy at 171°W, 16°30′S during the week of March 7–13, 2004 (the 'southern eddy'; Fig. 1), moved west–northwest about 60 km $week^{-1}$ and by 2 weeks had weakened so that the SSH at its core was approximately 10 cm higher than that depicted in Fig. 1. On another note, the main Samoan islands were engulfed by a relatively strong, short-lived (≤1 week) anticyclonic eddy that appeared on SSH averages a week prior to the conditions depicted in Fig. 1 (February 29 through March 6). Furthermore, the large cyclonic eddy centering on 165°W, 13°30′S during the week of March 7–13 (the 'northern eddy'; Fig. 1) was double in size with a core about 10 cm lower than a week earlier – engulfing the cyclonic eddy at 169°30′W, 11°30′S – with its signature completely gone from the SSH averages by 2 weeks later (from March 21 to 27, 2004). During the same 4 weeks (from the week of February 29 to March 6 to the week of March 21–27), a high sea surface anomaly appeared at the northern edge of the EEZ, moving east–southeast, and by 2 weeks after the week of March 7–13 (Fig. 1) covered a 6° × 2° area on the northeast corner of the map.

Typically, relatively high SSH during the months of March and April in the northern half of the EEZ identify the seasonally varying SECC, which cuts across that area (e.g. Fig. 2, left panels). However, during the rest of the year, when the kinetic energy of the SECC diminishes (Qiu and Chen, 2004), SSH drops about 30 cm in the northern part of the EEZ, resulting in relatively more uniform sea levels throughout the area (e.g. Fig. 2, right panels).

In addition to the seasonal variability of the SECC, the strength of the SECC shows interannual variability which affects the eddy activity in the study area. For example, during 2003, the seasonal variability in the SECC resulted in SSH variability – measured as the standard deviation (SD) of SSH – that more than doubled during the peak months relative to those during the rest of the year (Fig. 3a, solid line). This SD peak of 8.4 cm is relatively strong in comparison with the 7.2-cm mean SSH SD during the peak months of the last 10 years (1996 to 2005). In fact, only 2 years, 1998 and 2005, showed higher peak SDs than 2003, at 9.5 and 9.7 cm, respectively. The timing of these three strongest SSH SDs within the EEZ coincides with the last three El Niño events of the same 10-year period: the events in 1997–98, 2002–2003, and 2004–2005. However, the relative strengths of these three El Niño events were not reflected in the relative heights of the corresponding peak SSH SDs. The El Niño in 1997–98 was considerably stronger than the two other events, while the two highest SD peaks in the years 2005 (9.7 cm) and 1997 (9.5 cm) occurred during the weakest (2004–2005) and strongest (1997–98) El Niño years.

Figure 2. Mean sea surface heights over the American Samoa fishing grounds (top panels) and the EEZ (with geostrophic currents – bottom panels) for the months of March (left) and September (right). Top and bottom panels show data from the year of 2003 and averages over 2001 through 2004, respectively. High SSH on the left panels are the signature of the SECC. Note the wider color scale in the upper panels (also in Fig. 4) relative to the rest of the maps to accommodate for the higher SSH variability over the larger area. Moreover, notice the difference in scale for geostrophic currents on the lower panels.

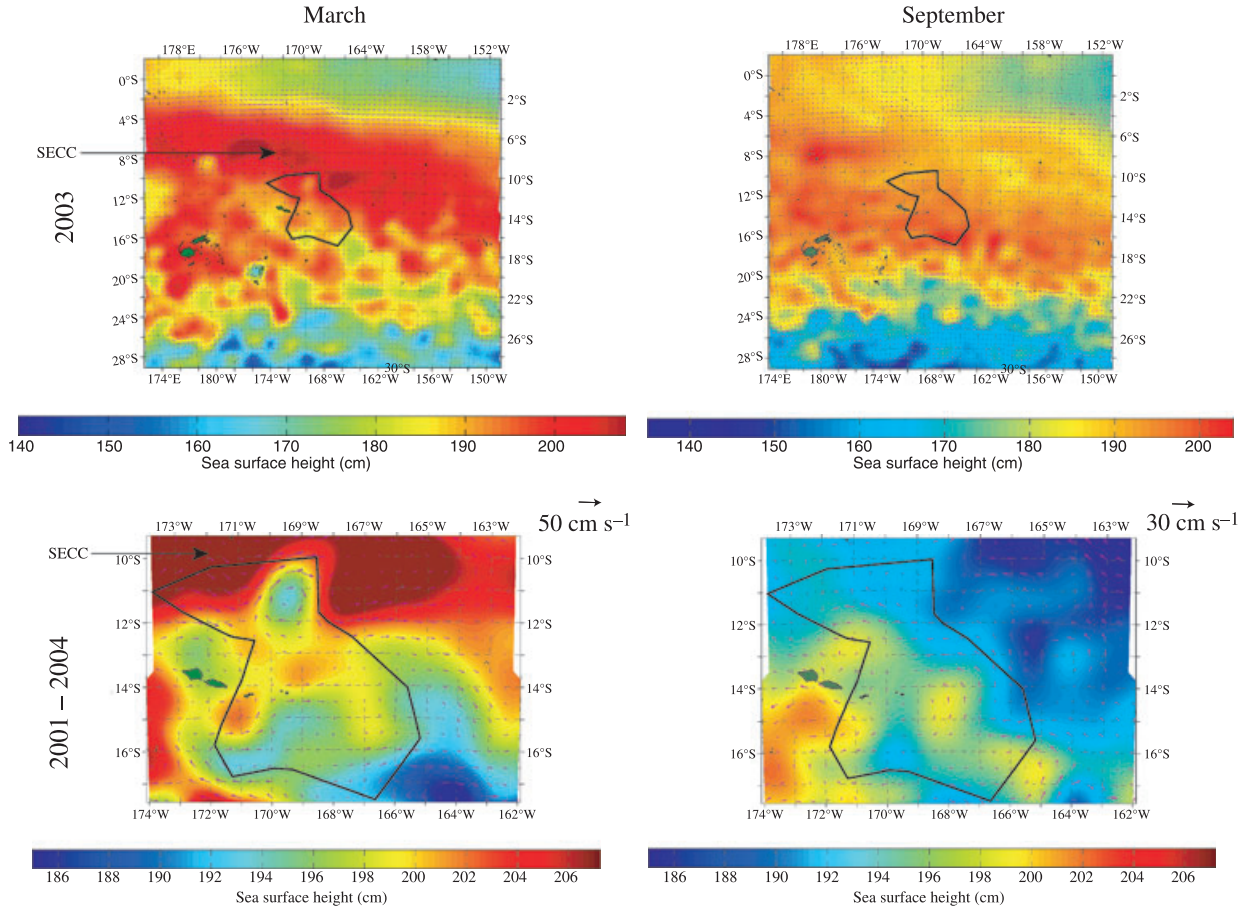

During 2004, the SECC velocities failed to intensify during the peak months as much as typically observed over the last 10 years. Slower currents in March and April 2004, relative to those in the typical years, resulted in the dissipation of the SECC kinetic energy west of the fishing grounds. Figure 4 shows the April SSH averages from 2003 (top) and 2004 (bottom), illustrating this effect. During the peak months of 2004, the relatively low kinetic energy levels of the SECC resulted in an approximately 20-cm drop in SSH in the northern part of the EEZ relative to those of the previous year (e.g., comparison of April 2003 with 2004 in Fig. 4 and the March mean values at bottom left in Fig. 2 to March 2004 in Fig. 1). The difference in eddy variability within the EEZ between the two years is illustrated in Fig. 3a.

Unlike SSH variability evidenced by the satellite altimetry data for the week of March 7–13, 2004, temperature profiles obtained from the CTD casts during March 3–13 exhibited little variability along and between the two meridional transect lines with no significant meridional nor zonal differences (Fig. 5). The mixed layer depth was approximately 70 m[1] below surface throughout both tracks, with the isotherms slightly shoaling toward north. Vertical sections of salinity showed a similar shoaling of the isohalines, although salinities exhibited a somewhat greater meridional variability. In addition, near-surface salinities were lower north of 14°S on the western and 12°S on the eastern transect than toward the south. The strongest temperature and salinity gradients within the thermocline appeared at depths of approximately 250 m. Unlike the temperature and

[1]Pressure in dbars ≅ depth in meters in the oceans.

Figure 3. Time series illustrating the seasonal and interannual variability in weekly sea surface height, albacore catch, and albacore CPUE (catch per 1000 hooks) over the EEZ, and their relationships to each other. (a) Standard deviations of sea surface heights for the years of 2003 (solid line) and 2004 (dashed line); (b) number of longline hooks (solid gray line) and number of albacore caught (dashed line) from January 1996 through February 2005; (c) standard deviation of sea surface height (solid gray line) and albacore CPUE (dashed line) for the year of 2003; (d) mean albacore CPUE (thick black line) and catch (thin gray line) averaged over the years of 2002 through 2004. Weekly catch and CPUEs are summed over time and the area of the EEZ.

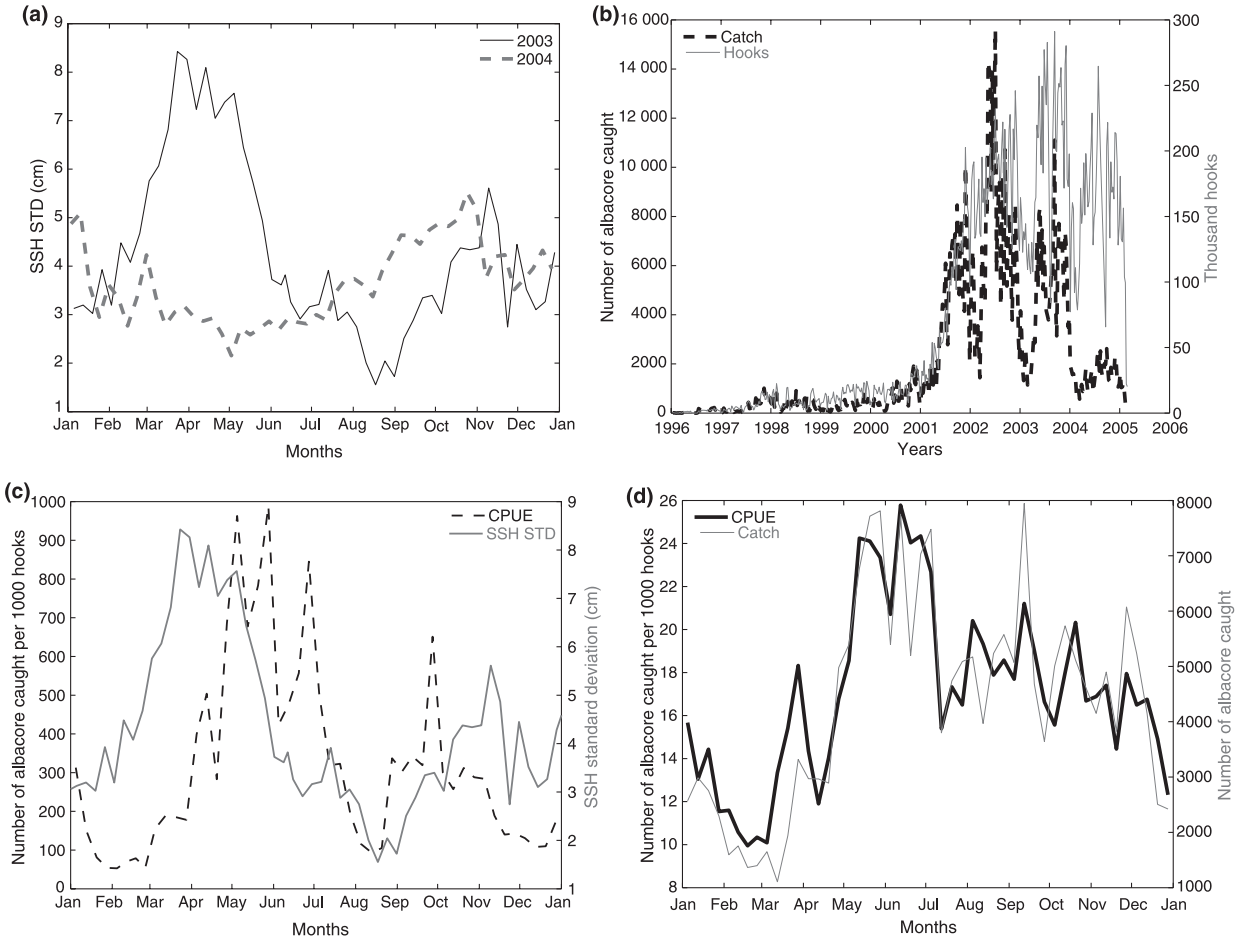

salinity distribution patterns, dissolved oxygen and chloropigments showed a meridional variability along both transects. Integrated dissolved oxygen values were generally higher south of 15°S for the western and south of 14°S for the eastern transects. Chloropigment maxima appeared at depths between 100 and 150 m, with a general increase in concentration from south to north. In addition, there was a sudden shallowing of chloropigment maxima to approximately 100 m below surface at the 11°30′S latitude, more prominent on the eastern transect, with an accompanying thickening of the layer and increasing concentrations. Furthermore, dissolved oxygen and chloropigments showed a zonal variability between the two transects. Dissolved oxygen values were generally higher while chloropigments were lower along the eastern transect relative to those along the western transect (Fig. 5).

Fishery performance and albacore distribution

The extraordinary growth of the American Samoa longline fishery, especially in 2001, is reflected in the time series of hooks set from the years of January 1996 to February 2005 (Fig. 3b, solid gray line). As Fig. 3b indicates, the number of hooks increased by about an order of magnitude from pre-expansion to postexpansion years. As stated earlier, this increase in the number of hooks is primarily a result of the introduction of larger vessels into the fishery that could travel farther from the islands than the small alia vessels and allow the use of larger sets. Most of the fishing activities in 1998,

Figure 4. Mean April sea surface heights and geostrophic currents for the American Samoa fishing grounds for the years of 2003 (top) and 2004 (bottom).

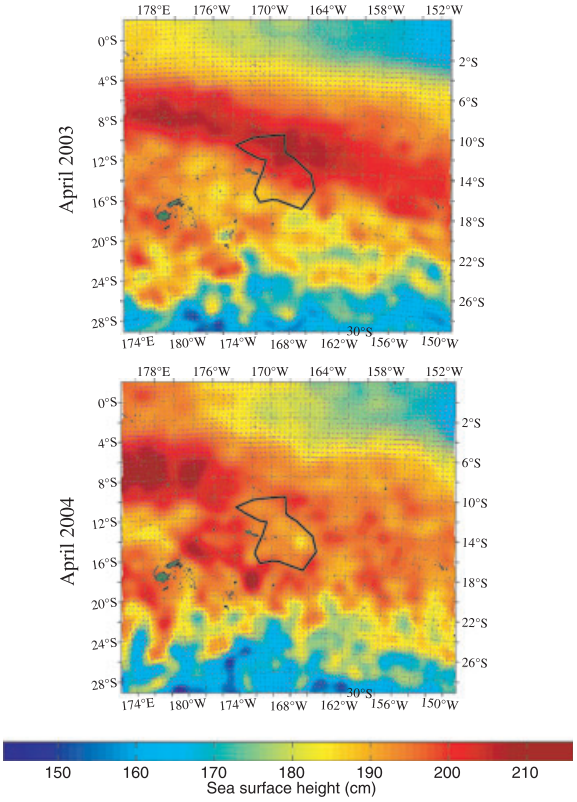

prior to the expansion, were confined to an area within a 30-km radius immediately to the southeast of the island of Tutuila, the main island of American Samoa, while by 2002, after the most intense expansion period, most hooks were set over a much larger – 10° longitude × 7° latitude – area (174–164°W, 17–10°S), with additional excursions to latitudes from 30°S to the equator. Because of this shift in both the composition of the longline fleet and the area being fished – as well as the insignificant number of hooks set prior to 2001 – data analysis in this study is focused on logbook records dated from January 2002 onwards, i.e. after the expansion.

As previous studies suggested that albacore are preferentially located in the high shear regions at eddy boundaries (e.g. Murphy and Shomura, 1972; Laurs and Lynn, 1977; Laurs *et al.*, 1984; Fiedler and Bernard, 1987), albacore catch and catch per unit effort (CPUE, measured as the number of albacore caught per 1000 hooks) locations were compared with the locations of relatively strong shear resulting from eddies and meanders within the EEZ. Maps showing weekly SSH and geostrophic currents with albacore catch and CPUE during the corresponding time periods reveal that albacore catches were predominantly located at the stronger shear regions of mesoscale features such as eddy boundaries or meanders, with higher CPUE associated with areas of stronger shear.

As an example, Fig. 6 shows the locations of albacore catches for the weeks of May 29 to June 5 (top) and August 14–21 (bottom), 2003, with the mean SSH and geostrophic currents for the same time periods. Most albacore catches were located at the boundary of eddies on both plots, with the highest albacore CPUE at the region of the strongest shear – as indicated by the geostrophic current velocities – during the week of May 29 to June 5. Furthermore, the overall albacore catch and CPUE were higher when the eddy variability was stronger in the EEZ (upper panel of Fig. 6) than when the eddy activity in the EEZ was diminished (lower panel of Fig. 6) in the absence of SECC influence (see Fig. 3a).

This seasonal variability in albacore catch rates and CPUE is the dominant trend for the post-expansion longline fisheries record. Averages of monthly albacore catch and CPUE, summed over the EEZ and averaged over the years from 2002 through 2004, show this seasonal pattern (Fig. 3d). Albacore CPUE rates nearly doubled during the months of May through part of July, relative to that during the rest of the year. The lowest catch and CPUE occurred during the month of February and the earlier part of March. The seasonal variability in albacore CPUE is associated with a seasonal variability in the spatial pattern of the number of hooks and CPUE as well. During the months of peak CPUE and the rest of July, the northern half of the EEZ is associated with significantly higher number of hooks and CPUE than the southern half (Fig. 7). The exceptionally high May 2003 northward CPUEs compared with the July 8-year averages reflect the relatively strong SECC in the peak months of 2003 as well as the absence of fishing vessels north of 14°S prior to 2001. Contrary to those observed in May through July, the CPUEs were considerably lower in the EEZ during the fall and winter months, without the northward skew observed during the peak months (e.g. the January mean values from 1996 through 2003; dashed thick line in Fig. 7). Instead, the highest CPUEs were observed near the island of Tutuila, approximately at 14°30′S, with the number of hooks evenly distributed over the EEZ. Note that the seasonal variability in albacore CPUE lags that of the SECC by about 2 months. For example, during 2003, the standard deviation of SSH in the region peaked in March through the beginning of

Figure 5. Temperature, salinity, dissolved oxygen, and chloropigments as measured by CTD casts along the 170°30′W (left) and the 169°00′W (right) meridians within the EEZ (see Fig. 1) from March 3 to 13, 2004.

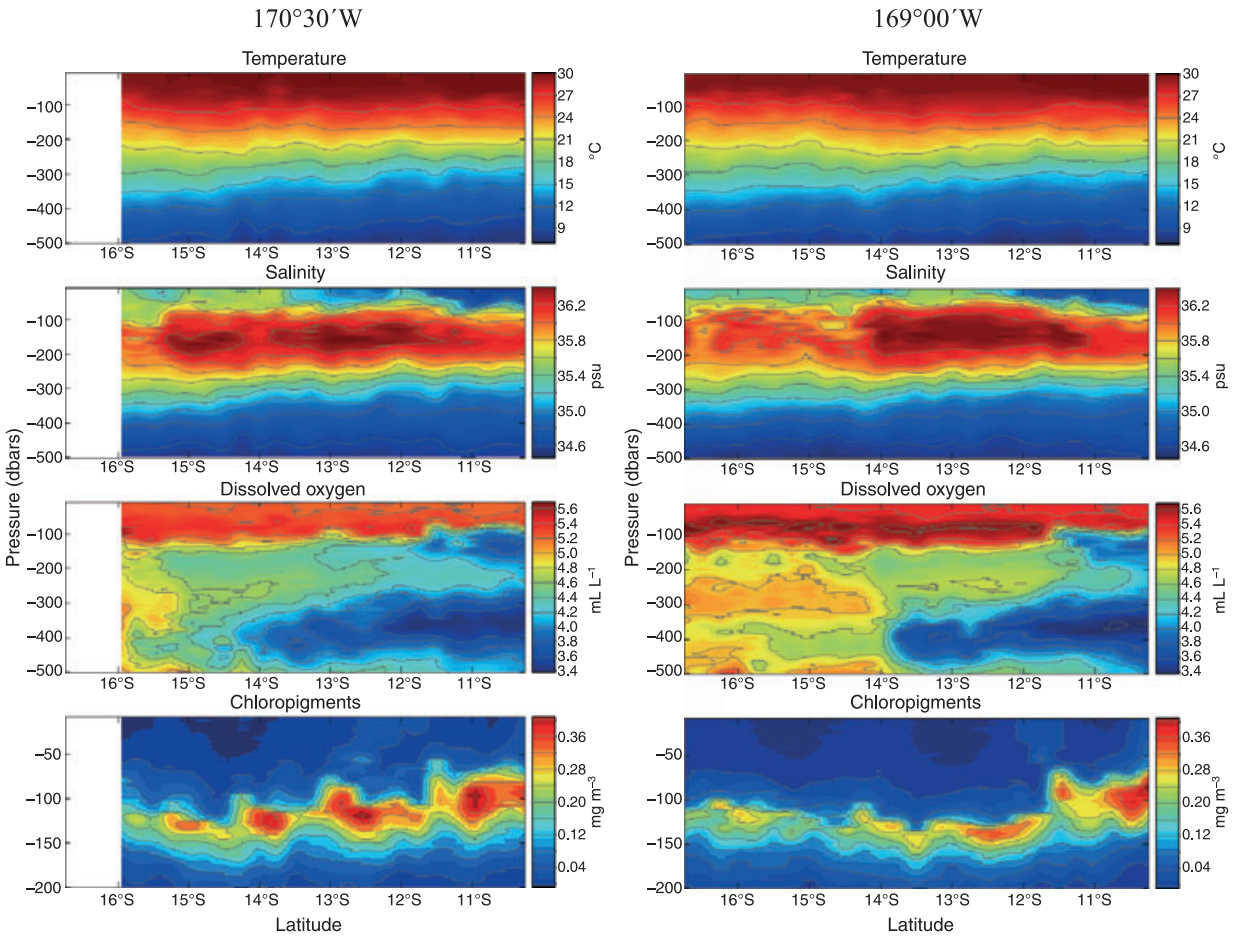

May, with the albacore CPUE peaking in May through the beginning of July (Fig. 3c).

In addition to the seasonal variability in albacore catch and CPUE, the performance of the longline fishery can vary from year to year. Figure 3b illustrates that while the number of hooks set does not change significantly from year to year during the post-expansion era, the catch (in numbers) dropped to near-pre-expansion levels during 2004. This dramatic drop in CPUE from 2003 to 2004 is accompanied by a lack of seasonal increase of CPUE from May through the beginning of July as well as a lack of northward skew in CPUE during this same time period and the rest of July (e.g. the month of May 2004; dashed thin line in Fig. 7). This lack of northward skew in CPUE during the peak months in 2004 is not reflected in the spatial pattern of the number of hooks, as they show a northward skew similar to those in 2003. Note that the lack of a seasonal increase and northward skew in albacore CPUE in 2004 coincides with the lack of seasonal eddy intensification in the region (Fig. 3a).

In addition to examining the horizontal distribution of albacore catches, the vertical distribution of albacore in the American Samoa EEZ was studied using depth and temperature records obtained from tagged albacore inside of the area of Box 1 (Fig. 1). Of the six tags set, only two ('albacore no. 1', with 95 cm fork length, and 'albacore no. 2', with 93 cm fork length) lived longer than a few days but nevertheless exhibited the diel migratory pattern expected of this species. The tag on albacore no. 1 gave 16.21 live-days (in 4-h bins) while the tag on albacore no. 2 gave 5.83 live-days (in 1-h bins).

Data obtained from the two successfully tagged albacore show a 5.5-km net horizontal displacement from the tag set to the tag pop-up locations: the tag on albacore no. 1 popped up 10.45 km west from its set location (170°36.2′W; 15°24.2′S versus 170°42.0′W; 15°24.6′S), giving an average of 645 m displacement

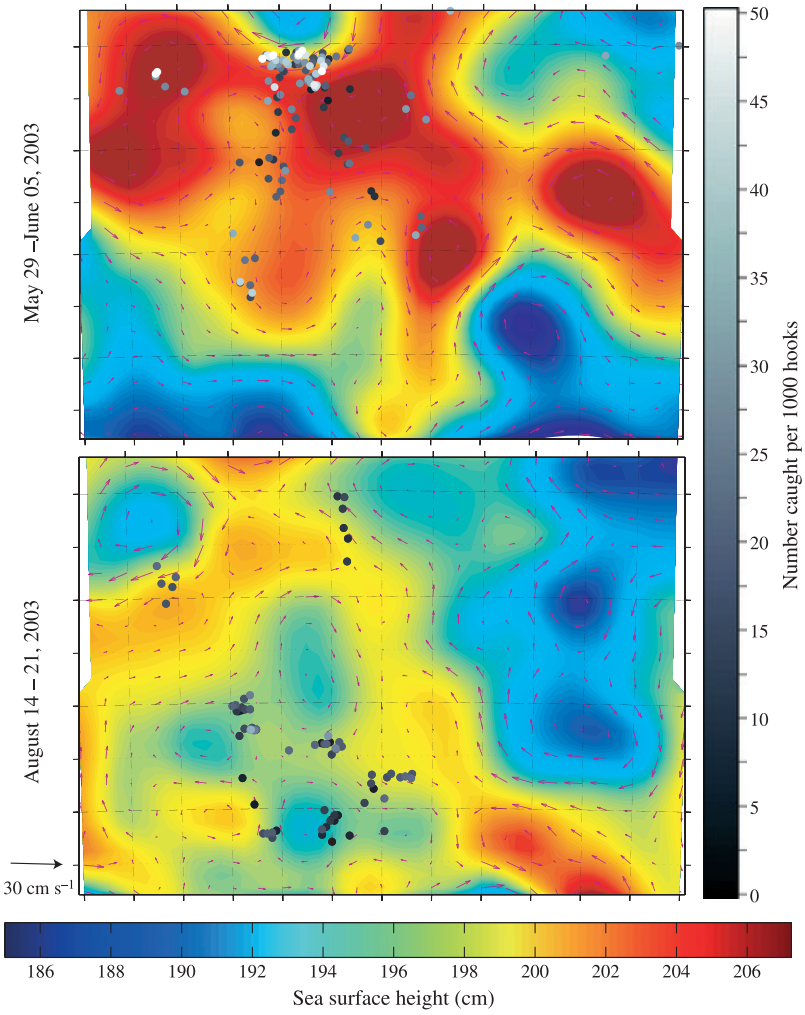

Figure 6. Albacore catch locations and CPUE (number caught per 1000 hooks) plotted over sea surface heights and geostrophic currents for the weeks of May 29 to June 5 (top) and August 14 to 21 (bottom), 2003. Note that because of privacy concerns, latitude and longitude labels are omitted on these plots.

per day, while the tag on albacore no. 2 popped up 520 m west–northwest from its set location (170°22.5′W; 15°30.7′S versus 170°22.8′W; 15°30.6′S), giving an average of 89 m displacement per day. This net horizontal displacement of individuals while tagged was only a fraction of the 31.6-km net distance between the two albacore at the time of tagging and at the time of the pop-up of the tags (27.20 and 36.05 km for tagging and pop-up, respectively).

Depth and temperature records from albacore no. 1 and no. 2 show a depth range of 0–300 m below the surface, with corresponding temperatures of 30 to 18°C. On average, the two albacore spent most of their time (75% and 60% for albacore no. 1 and no. 2, respectively) in the 150–250 m depth range, in 25–20°C waters. Depth and temperature records obtained from the 18 TDRs attached to three commercial longline sets during the time, and within the area of the tagging operations (February 29 to March 2, 2004, within Box 1 – see Fig. 1) all showed settling depths and temperatures that correspond to those recorded by the two successful tags: 100–380 m depth and 28–13°C temperature.

Depth and temperature records from the pop-up tags attached to the albacores indicated diel vertical movement patterns typical for albacore tuna: at night both albacore stayed closer to the surface (but still below the mixed layer depth), descending to deeper waters during the daytime. To examine this diel vertical migratory pattern, the time spent by each albacore was separated into day and night blocks, with daytime and nighttime defined as 08:00–17:00 and 20:00–05:00 hours, respectively, attempting to be consistent with the sonic scattering layer observations (see succeeding section). During the daytime, both albacore stayed in the 150–300 m depth range (Fig. 8, top left panel), in waters with temperatures ranging from 25 to 18°C. Albacore no. 1 spent most of its time (72%) in the 200–250 m depth bin, while albacore no.

Figure 7. Latitudinal distribution of albacore CPUE (number caught per 1000 hooks) for the months of July (solid thick line) and January (dashed thick line), averaged over the years of 1996 through 2003, and for the month of May in 2003 (solid gray line) and 2004 (dashed gray line). CPUE are summed over each month and 0.25° latitude.

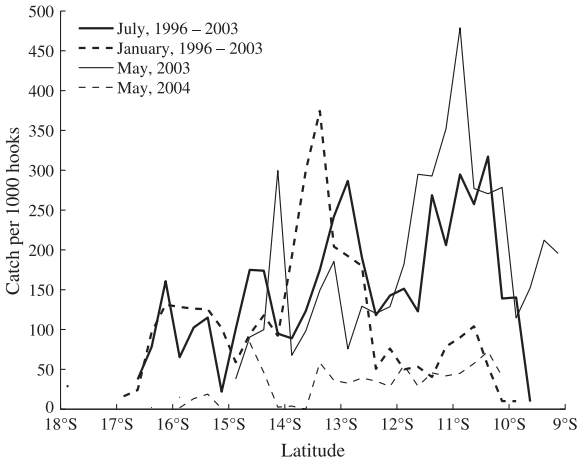

2 spent 70% of its time at approximately 200 m depth (47% in the 150–200 m and 23% in the 200–250 m depth bins). Both albacore tuna spent the rest of their time mostly in the 250–300 m depth bin during the day. During the night, both albacore tuna occupied depths of 0–200 m (Fig. 8, top right panel), with temperatures ranging between 30 and 24°C. Albacore no. 1 and no. 2 spent 58% and 41% of their time in the 100–150 m and the 150–200 m depth bins, respectively, occupying mostly shallower depths the rest of the time. Neither albacore dove below 250 m during the nighttime.

Characteristics of the sonic scattering layer

The most prominent feature of the acoustic backscatter is the diurnal pattern of the vertically migrating sonic scattering layer (SSL). During the daylight hours the strongest acoustic backscatter was found in the 500–800 m depth range (deep scattering layer) and during the night in the 10–150 m depth range (shallow scattering layer). Both dawn and dusk transition times typically last longer than 1.5–2 h but can deviate up to 45 min in response to changes in light levels as a result of environmental factors (e.g. cloud cover, moonlight). The SSL is predominantly composed of several thin layers which become most prominent during transition times as the migratory organisms that compose the SSL start and end their vertical migrations asynchronously.

To examine the mean daytime and nighttime vertical patterns of the backscatter within the EEZ, both daytime and nighttime mean NASC obtained over the two transects (see Fig. 1) were horizontally averaged for the 38- and 120-kHz channels. These averages show the strong nighttime (Fig. 8, left panels) SSL in the upper 200 m, with daytime averages increasing with depth from 350 m as nearing the depth of the daytime SSL. Typically, NASC values at 38 kHz (Fig. 8, top panels) are higher than at 120 kHz (Fig. 8, bottom panels) with some exceptions (e.g. at around 180 m during nighttime), although the differences between the two are more pronounced during night than during the day. Both day and night plots show persistent local maxima at 250 m, and at 120 and 200 m, respectively. As Fig. 8 illustrates, the depths of the local daytime and nighttime NASC maxima correspond to the depths at which the two tagged tuna spent most of their time: in the 150–200 and 200–250 m depth bins during the day and in the 100–150 m and 150–200 m bins during the night.

In addition to examining the vertical pattern of the bioacoustic scattering, NASC values from both frequencies were integrated over the upper 200 m to examine their meridional and zonal characteristics within the EEZ. One of the prominent features of the integrated upper 200-m scattering is the spatial variability in the strength of area-scattering coefficients at both the 38- and 120-kHz frequencies (Fig. 9). While the 38-kHz NASC values are typically higher – especially during night – than those of the 120 kHz (as observed previously), there are spatial differences in both the NASC values and their ratios at both frequencies. During daytime, the 120-kHz NASC values frequently exceeded those of the 38-kHz approximately twofold (compare Fig. 9 top and bottom left panels). However, near the island of Tutuila (13–15°S on the western transect) the 38-kHz integrated NASC are more than three times those of the 120-kHz ($\sim$350 versus $\sim$100 m^2 nmi^{-2}). During nighttime, the integrated values at 38 kHz were about twice those at the 120-kHz frequency ($\sim$600 versus $\sim$300 m^2 nmi^{-2}) with the 120-kHz NASC never exceeding the NASC at 38 kHz (compare Fig. 9 top and bottom right panels – note the differences between daytime versus nighttime and nighttime 38-kHz versus 120-kHz NASC color scales). As opposed to daytime, during the night the western transect showed relatively high NASC values south of 15°45′S at both frequencies.

There does not seem to be a spatial correspondence between the weekly SSH records and the integrated upper 200-m NASC values, except the relatively high NASC values on the western transect south of

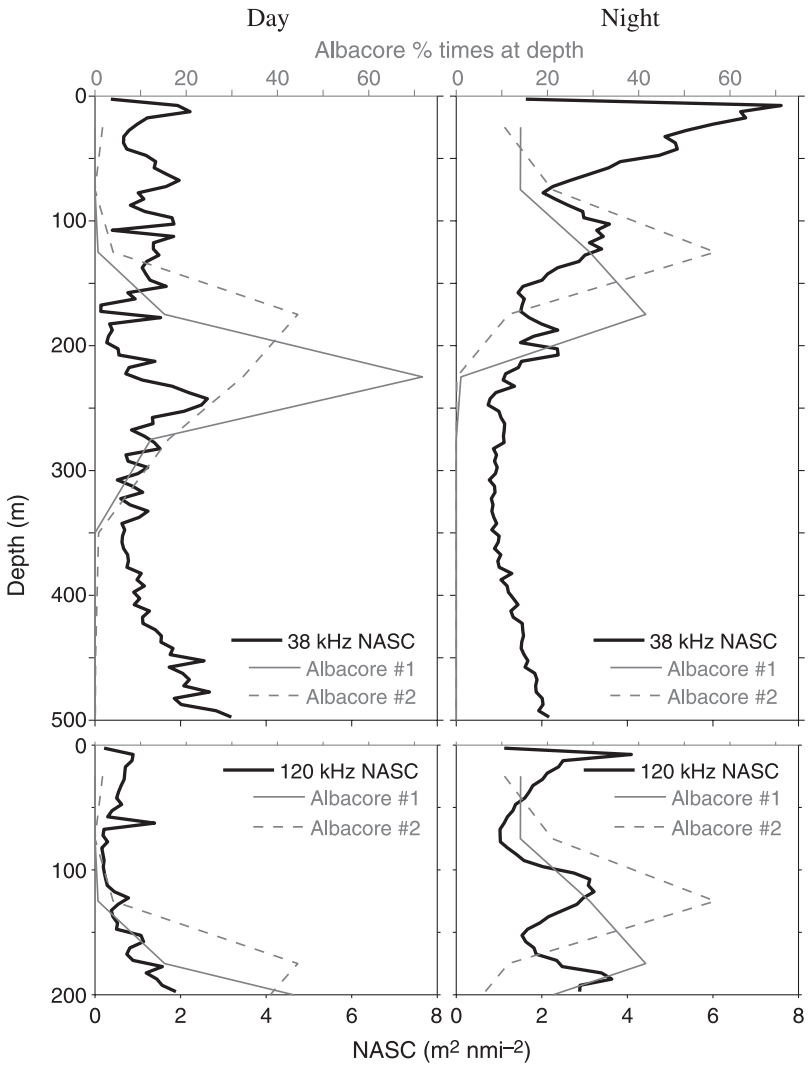

Figure 8. Percent time spent at depth by two tagged albacore (solid and dashed gray lines for albacore no. 1 and no. 2, respectively), with the horizontally averaged nautical area scattering coefficients (solid thick line) at 38 kHz (top) and at 120 kHz (bottom), during daytime (left) and nighttime (right). Tag durations for albacore no. 1 and no. 2 are ~16 and ~6 days, respectively.

15°45′S at both frequencies (Fig. 9). This feature seems to correspond to relatively high shear at the northeast boundary of a cyclonic eddy (the southern eddy), inferred from the low sea surface heights and the relatively strong geostrophic currents in that location.

A prominent zonal feature of the integrated upper 200-m scattering coefficients is the persistently higher NASC values over the western transect as opposed to those at the eastern transect both during the day and night and at both frequencies (Fig. 9). This westward intensification of scattering coincides with lower dissolved oxygen and higher chloropigment concentrations toward the west relative to the east (Fig. 5). Note, however, that in the absence of CTD data toward the southern end of the western transect, the nighttime intensification of the upper 200-m scattering below 15°45′S and over the western transect, observed at both frequencies, could not be compared with dissolved oxygen and chloropigment concentrations.

DISCUSSION

The results of this study show that the American Samoa EEZ is a dynamic region with mesoscale oceanographic activity exhibiting temporal variability on scales less than a week. The American Samoa EEZ – especially its northern half – is heavily influenced by both the seasonally and interannually variable SECC, resulting in increased eddy activity when the kinetic energy of the SECC is at its strongest. The timing of the three strongest SSH anomalies suggests that El Niño events might have an influence on the interannual variability of the SECC – and the resulting eddy activity in the region.

Figure 9. Depth-integrated nautical area scattering coefficients and mean sea surface heights for the week of March 7–13 during daytime (left) and during nighttime (right) for the 38 kHz (top) and 120 kHz (bottom) frequencies. The integration interval is from 0 to 200 m in depth. Note the change in color scale: for daytime, NASC is 0–300 m^2 nmi^{-2} for both frequencies, while for nighttime, NASC is 0–800 m^2 nmi^{-2} for the 38-kHz and 0–400 m^2 nmi^{-2} for the 120-kHz channel.

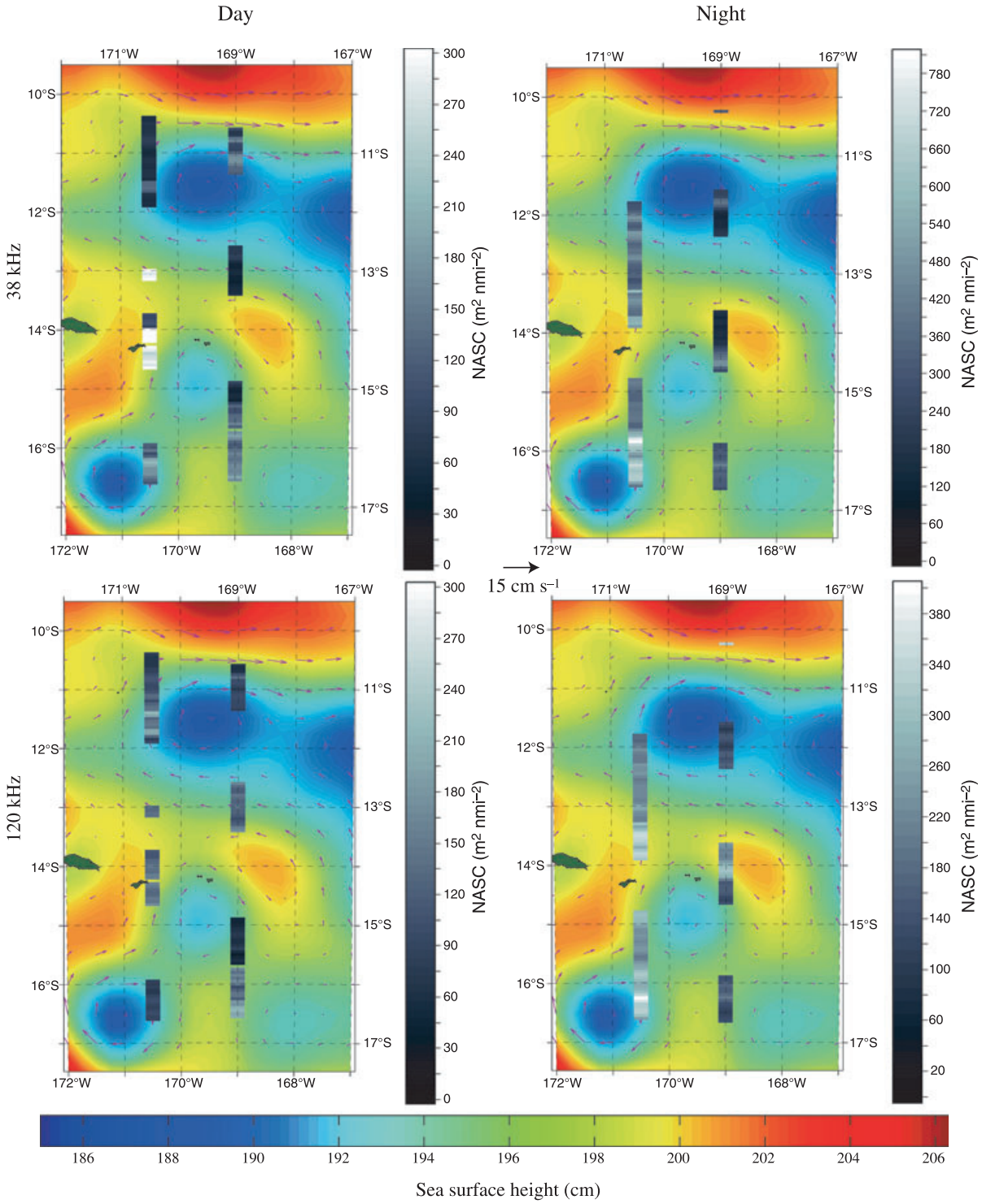

In turn, this variability in eddy activity appears to have a strong influence on the performance of longline fisheries for albacore, *T. alalunga*, although the length of the logbook time series is not sufficient to establish a definitive connection. Furthermore, elevated CPUE in the area of increased eddy activity likely indicates increased biomass of albacore, even though catch per effort does not necessarily translate into fish abundance at a certain location. However, this observation is consistent with expectations based on previous studies showing the preferential aggregation of large pelagic fish, such as tuna, in areas of increased shear associated with mesoscale eddies (e.g. Murphy and Shomura, 1972; Fiedler and Bernard, 1987; Seki *et al.*, 2002).

To determine whether albacore move into the area of the EEZ with the SECC or if it aggregates from ambient waters during the peak months of May through the early part of July is outside of the scope of this study. Nevertheless, it seems that longline fishers have observed, and still use to their advantage, the seasonal trend, as indicated by the elevated number of hooks set – as well as the tendency to occupy the northern half of the EEZ – from May to July (Fig. 7). It is interesting to note, however, that while most of the year the fleet stays within the boundary of the EEZ, during March and April, when the kinetic energy of the SECC is strongest with its effects extending to the east of the EEZ, a significant portion of the hooks are set at around 2°S, 162°W, to the north of the EEZ as well as to the stronger sheer associated with the boundary region between the SEC and SECC. It is possible that some of the fishing vessels move north to take advantage of the equatorial current system, as the fishery performance within the EEZ is low during this time (Fig. 3d). Note, however, that higher catch rates do not necessarily reflect higher tuna abundance but could indicate higher catchability if, for example, albacore is distributed at shallower depths near the equator, allowing for longline fishers to sample its entire vertical range. Another time period when the fleet tends to leave the EEZ is the months of August and January, when both the kinetic energy of the SECC and the fishery's performance are at a low. During these months, a significant number of hooks is set at around 25°S, 170°W, south of the EEZ.

The results of this study cannot confirm a definitive link between increased micronekton biomass and high shear regions associated with eddy edges. Although the nighttime SSL increases at the boundary region of the southern cyclonic eddy, no such increase can be seen at the edges of the northern cyclonic eddy (Fig. 9). This apparent lack of a clear effect on micronekton biomass is consistent with other findings (e.g. Ménard *et al.*, 2005) and is not entirely surprising. Most micronektonic organisms exhibit the diel vertical migratory pattern, occupying depths below the influence of mesoscale eddies during the day. The apparent lack of the northern eddy's influence on micronekton biomass could also be a result of the fact that it is a relatively short-lived, fast-moving eddy formed only 1 or 2 weeks prior to the time of the SSL measurements. It is conceivable that the accumulation of micronekton biomass may require more than a couple of weeks. The southern eddy, on the other hand, had formed several weeks before the SSL measurements were obtained, possibly allowing for the accumulation of micronekton at its boundary region. The 2-month lag between the peak times of eddy activity and CPUE within the EEZ could reflect the accumulative response times for the micronekton and albacore tuna, assuming that the increase in CPUE is attributable to the preferential aggregation of albacore in response to the accumulation in micronekton biomass. Also noteworthy, during the time of the SSL measurements (March 3–13, 2004), the fleet was concentrating on the northern edge (~12°S 172°W) of the dissipating anticyclonic eddy engulfing the main Samoa islands, with some of the hooks (and albacore catch) at the southern edge of the northern cyclonic eddy (~12°S; 169°30′W). CPUE did not exceed 10 albacore per 1000 hooks for any individual set, giving significantly lower values than those during off-season times in 2003 (see Fig. 6b).

In contrast to the lack of observed effects of the northern eddy on the micronekton distribution, changes in chloropigment and dissolved oxygen concentrations along both transects at latitudes coinciding with those of the northern eddy are consistent with expected signatures of cyclonic eddies. However, temperature and salinity records indicate the lack of anticipated upwelling in that area (Fig. 5). Regardless, the increased concentrations of chloropigments could enhance secondary production, which, in turn, could cause the observed drop in the dissolved oxygen concentrations shown in Fig. 5. The assumption of a causal relationship between the two is strengthened by the close match between the bottom contours of high concentrations of dissolved oxygen and the top contours of high concentrations of chloropigments along both transects (note that the depth scales for dissolved oxygen and chloropigments are 0–500 m and 0–200 m, respectively).

The lack of an observable upward shift of the isotherms at the location of the northern eddy is puzzling,[2] although the lack of sea surface temperature change is typical for short-lived eddies that are formed by barotropic instability from relatively homogeneous water masses. As opposed to boundary current eddies, these mid-ocean eddies do not necessarily have sea surface temperature signatures, for they are formed from water masses with similar characteristics. As the SECC originates to the east of Papua New Guinea in the South Pacific Convergence Zone (SPCZ) – and approximates the SPCZ's route to Fiji – its water mass is expected to contain high near-surface temperatures with low salinities. It is likely that the SECC helps advect and sustain the low sea surface salinity tongue to the east, indicated in Fig. 5 by the low near-surface salinities north of 14°S and 12°S along the western and eastern transects, respectively. The difference in the meridional extensions of the low-salinity water between the two transects could indicate the advection of the low-salinity tongue from the west to the east. The differences between the SECC and SEC water masses could also be responsible for the increase in dissolved oxygen and decrease in chloropigment concentrations from the west to east.

The increase in chloropigment concentrations from east to west coincides well with a decrease in dissolved oxygen concentrations and with an increase in the upper 200-m SSL both during daytime and nighttime and at both frequencies (cf. Figs 5 and 9). Increased concentrations of chloropigments represent higher phytoplankton concentrations, allowing for an increase in the biomass of zooplankton and possibly micronekton. The lower concentrations of dissolved oxygen could be the result of higher biomass of micronekton (and, presumably, zooplankton) along the western transect relative to those that are along the eastern transect.

In general, the vertical distribution of the SSL is consonant with previous observations in the vicinity of the American Samoa EEZ. As part of the ECOTAP Program, Bertrand *et al.* (1999) observed the shallow and deep SSL above 200 m and between 500 and 800 m depths, respectively, in the French Polynesian EEZ – about 20° east from the American Samoa EEZ. As observed in the present study, Bertrand *et al.* also found local maxima in backscattering strength, although lying at 200–300 m depth, 50 m deeper than the 150–250 m deep maxima in the American Samoa EEZ.

Changes in the relative composition of the shallow SSL can be inferred from the differences in the relative backscattering coefficients at the two frequencies, even though the SSL gives stronger returns in general at the 38-kHz relative to those at the 120-kHz frequency. These overall higher 38-kHz NASC values agree with expectations based on the scattering properties of the organisms likely to make up the SSL in the area. Bertrand *et al.* (2002b) found that in waters bordering the American Samoa fishing grounds on the east (the French Polynesian EEZ at 4–20°S; 154–134°W) – fish, particularly myctophids, make up about 70% of the SSL, with the rest composed of 10% cephalopods (mainly squid), 13% crustaceans (mainly euphausiids), and 7% gelatinous organisms. The predominance of myctophids in the South Pacific has been shown by other authors as well (e.g. Young *et al.*, 1996). Although myctophids, as well as other small fish, are expected to make up most of the backscattering energy at both frequencies because of their swimbladder (Foote, 1980) and their dominance in the scattering layer, they are also expected to scatter stronger at the 38-kHz than at the 120-kHz frequency (MacLennan and Simmonds, 1992). Cephalopods have target strengths within the same range as those of myctophids at 38 kHz (e.g. Kajiwara *et al.*, 1990; MacLennan and Simmonds, 1992) and give equal (Goss *et al.*, 1998) or slightly higher (Goss *et al.*, 2001) returns at 120 kHz. On the other hand, gelatinous organisms have been shown to have high backscattering strengths at 38 kHz which become insignificant at the 120-kHz frequency (Benoit-Bird and Au, 2001; Brierley *et al.*, 2004), while euphausiids (as well other plankton) scatter stronger at the 120-kHz than at the 38-kHz channel (e.g. Everson *et al.*, 1993; McKelvey, 2000; Swartzman, 2001; Ressler *et al.*, 2004; Demer and Conti, 2005).

Based on these scattering properties of the organisms composing most of the SSL, the overall higher NASC values at the lower frequency are consistent with the hypothesis of a predominance of small fish (and possibly cephalopods) in the upper 200-m SSL. The observed patchiness in the differences in the horizontal (Fig. 8) and vertical (Fig. 9) averages of the relative backscattering strengths at the two frequencies is indicative of both vertical and horizontal changes in the relative composition of the SSL. The greater nighttime differences in NASC at the two frequencies, as well as the persistence of the deep scattering layer, could indicate that mostly organisms

[2]To confirm the accuracy of the SSH records, dynamic heights and geostrophic currents were calculated from the *in situ* temperature and salinity records. These *in situ* dynamic heights and geostrophic currents are consistent with those from the satellite record.

in the deep scattering layer that scatter stronger at the lower frequency – such as fish, squid, and gelatinous organisms – migrate to shallower depths during nighttime.

The vertical distribution of albacore tuna seems to be strongly influenced by the availability of food, although the sample size of two successfully tagged albacore is clearly not adequate for a definitive conclusion. While the two tuna preferred the SSL local maxima at 150 and 250 m, they did not spend much of their time either at the near-surface nighttime NASC maximum or in the deep daytime SSL (Fig. 8). These observations are consistent with the findings of the ECOTAP Program in the French Polynesian EEZ, where the vertical (and horizontal) distribution of albacore and other tunas are correlated with dense patches of micronekton at the 200–300 m depth range (e.g. Josse *et al.*, 1998; Bertrand *et al.*, 2002a,b). It is possible that in the American Samoa EEZ, the albacore prefer the composition of prey species at the 150–250 m depth range, where the relative backscattering strengths at the two frequencies indicate a higher percentage of crustaceans and probably cephalopods than within the upper 20-m layer. Albacore's preference of micronekton layers with relatively higher concentrations of crustaceans and cephalopods is in accord with studies involving albacore stomach content analyses in French Polynesia. Based on data from 2001 to 2005, M-L. Coudron (unpublished data; contact D.S. Kirby, Secretariat of the Pacific Community, Noumea, New Caledonia) found that crustaceans and mollusks made up 62% of albacore's stomach contents (31% each), as opposed to the mostly fish-based diet of bigeye and yellowfin tuna. It is interesting to note, however, that Bertrand *et al.* (2002a) found that albacore's stomachs contained roughly 50–60% cephalopods, 35% fish, and 10% crustaceans in the French Polynesian EEZ during 1995–97. This apparent change in the diet of albacore is in agreement with findings from another study (D.S. Kirby, Secretariat of the Pacific Community, Noumea, New Caledonia, pers. comm.)[3] indicating that from 1995–97 to 2001–2004, there was a 46% increase and a 10% decrease in epipelagic crustaceans and mesopelagic squids in albacore's stomach contents from French Polynesia, accompanied by a 42% decrease in fish diversity. As Kirby postulates, it is possible that changes in the environment are responsible for the changes in prey availability, and, as a result, in the diet of albacore.

Neither oxygen nor temperature seems to be limiting factors in the albacore's avoidance of the shallow and deep SSL, although temperature might play some role. Bertrand *et al.* (2002b) reports that 97.5% of all experimental longline albacore catch in the French Polynesian EEZ occurred in waters with dissolved oxygen concentrations and temperatures above 1.5 mL L^{-1} and 10°C, respectively. In the American Samoa EEZ, the dissolved oxygen minimum, 3.4 mL L^{-1}, is at 400 m depth (Fig. 5), only slightly below the albacore's preferred concentrations at 3.7 mL L^{-1} (Graham *et al.*, 1989); but within the deep SSL, dissolved oxygen concentrations are consistently above 4.0 mL L^{-1}. Furthermore, dissolved oxygen concentrations in the area of Box 1, enclosing both tags' set and pop-up locations (between 15°15.4′S and 15°32.9′S on the western transect), are above 4.5 mL L^{-1}, with a maximum of 5.8 mL L^{-1} in the 550–750 m depth range. These findings indicate that dissolved oxygen is not likely to be a limiting factor for albacore in the American Samoa EEZ. However, at the depth of the deep scattering layer (500–800 m), the temperature drops below the 10°C minimum temperatures reported by Bertrand *et al.* (2002b). Note that in this study, the two tagged albacore spent most of their time at 150–250 m depths with temperatures between 20 and 25°C, not spending time at 300–500 m depths where the temperature was between 19 and 10°C. As opposed to these temperature ranges, albacore in the northeast Pacific (~40°N) have been observed to occupy waters with 10–17°C temperatures (e.g. Laurs, 1983; Laurs and Dotson, 1992), corresponding to a depth range of 150–250 m, the same depth range as in this study.[4] While it is possible that south Pacific albacore prefer warmer waters than albacore from other Pacific locations, their similar depth distribution and their avoidance of shallower waters might point to the importance of food as a governing factor in the vertical distribution of albacore.

It is interesting to note that the three longline sets tested in this study show settling depths similar to the depths where the two tagged albacore spent most of their time, presumably feeding. Bertrand *et al.* (2002b) found albacore catch rates to be persistently lower at depths of dense micronekton patches than at depths relatively devoid of prey – presumably because albacore

[3]See http://www.soest.hawaii.edu/PFRP/nov06mtg/kirby.pdf.

[4]Note that in Bertrand *et al.*'s (2002b) study, albacore mean weight was 20.7 kg, comparable with fork lengths ~97 cm and to the sizes of albacore in the present study, while Laurs (1983) and Laurs and Dotson (1992) include data obtained from juvenile to adult albacore in their analyses.

avoid bait in the presence of abundant forage. Note that during the time of this study, March 2004, eddy activity (as well as albacore CPUE) was at a relative low (Fig. 3a). It is possible that during stronger eddy activity, the stronger currents result in shallower settling depths that are relatively devoid of prey. The reported higher incidental catch of typically shallower dwelling fauna during 2002–2003 is indicative of shallower settling depths than those observed at the time of this study. Fishing at shallower depths where albacore are more attracted to bait might help raise CPUE at the time of enhanced eddy activity (e.g. compare SSH SD and albacore CPUE during May 2003, to those during May 2004, on Figs 3a and 7).

The results of this study imply that albacore may be less migratory than is generally thought, or that their migratory behavior is confined by environmental factors. Although no position readings are available between tagging and pop-up locations, the net daily displacements of 645 and 89 m for albacore no. 1 and no. 2 – along with the much longer distances between the two albacores at the times of tagging (27.20 km) and pop-up (36.05 km) – suggest that they spent most of their time foraging, without transiting horizontally through space.

While leaving many questions unanswered, this study provides strong support for the importance of the SECC to the performance of the local fishery for albacore, as well as essential information on albacore and micronekton movement patterns and distribution in the American Samoa EEZ. This study serves as the first step in the characterization of the American Samoa albacore tuna habitat and fishing grounds, a poorly studied region. Although preliminary, the results presented here provide valuable information for directing future research on the oceanographic characterization of this economically important area.

ACKNOWLEDGEMENTS

The authors acknowledge the help and support of many who made this project possible. We thank the officers and crew of the NOAA ship, *Oscar Elton Sette*, for their work and dedication to the success of this study. Evan Howell provided PAT tag and, together with Lucas Moxey, satellite remote sensing data support. Shuiming Chen engaged in instrumental discussions on the characteristics and effects of the South Equatorial Counter Current. D. Curran, R. Domokos, D. Hawn, K. Hogrefe, and C. Musburger participated on the shipboard survey. This project was supported by the JIMAR Pelagic Fisheries Research Program of the University of Hawaii School of Ocean and Earth Science and Technology under Cooperative Agreement number NA17RJ12301 from the National Oceanic and Atmospheric Administration.

REFERENCES

Anonymous (2002) Fisheries off west coast states and in the Western Pacific; pelagic fisheries; prohibition on fishing for pelagic management unit species; nearshore area closures around American Samoa by vessels more than 50 feet in length, Final Rule. (U.S.) Federal Register, 67, pp. 4369–4372.

Benoit-Bird, K.J. and Au, W.W.L. (2001) Target strength measurements of Hawaiian mesopelagic boundary community animals. *J. Acoust. Soc. Am.* **110:**812–819.

Bertrand, A., Le Borgne, R. and Josse, E. (1999) Acoustic characterization of micronekton distribution in French Polynesia. *Mar. Ecol. Prog. Ser.* **191:**127–140.

Bertrand, A., Bard, F.X. and Josse, E. (2002a) Tuna food habits related to the micronekton distribution in French Polynesia. *Mar. Biol.* **140:**1023–1037.

Bertrand, A., Josse, E., Bach, P., Gros, P. and Dagorn, L. (2002b) Hydrological and trophic characteristics of tuna habitat: consequences of tuna distribution and longline catchability. *Can. J. Fish. Aquat. Sci.* **59:**1002–1013.

Bigelow, K., Musyl, M.K., Poisson, F. and Kleiber, P. (2006) Pelagic longline gear depth and shoaling. *Fish. Res.* **77:**173–183.

Boggs, C.H. (1992) Depth, capture times, and hooked longevity of longline-caught pelagic fish: timing bites of fish with chips. *Fish. Bull. U.S.* **90:**642–658.

Brandt, S.B. (1981) Effects of warm-core eddy on fish distributions in the Tasman Sea off East Australia. *Mar. Ecol. Prog. Ser.* **6:**19–33.

Brierley, A.S., Axelsen, B.E., Boyer, D.C. *et al.* (2004) Single-target echo detections of jellyfish. *ICES J. Mar. Sci.* **61:**383–393.

Collette, B.B. and Nauen, C.E. (1983) *FAO Species Catalogue, Vol. 2, Scombrids of the World*. FAO Fish. Synop. 2, pp. 137.

Demer, D.A. and Conti, S.G. (2005) New target-strength model indicates more krill in the Southern Ocean. *ICES J. Mar. Sci.* **62:**25–32.

DMWR. (2002) American Samoa Department of Marine and Wildlife Resources (DMWR) Report on the NMFS Logbook Program for the American Samoa Longline Fishery, October–December 2001, p. 6.

Everson, I., Goss, C. and Murray, W. (1993) Comparison of krill (*Euphausia superba*) density estimates using 38 and 120 kHz echosounders. *Mar. Biol.* **116:**269–275.

Fiedler, P.C. and Bernard, H.J. (1987) Tuna aggregation and feeding near fronts observed in satellite imagery. *Continental Shelf Res.* **7:**871–881.

Foote, K.G. (1980) Importance of the swimbladder in acoustic scattering by fish: a comparison of gadoid and mackerel target strengths. *J. Acoust. Soc. Am.* **67:**2084–2089.

Gill, A.E. (1982) *Atmosphere-Ocean Dynamics*. W.L. Donn (ed.) San Diego: Academic Press, Inc., pp. 662.

Goss, C., Rodhouse, P.G., Watkins, J.L. and Brierley, A.S. (1998) Identification of squid echoes in the south Atlantic. *CCAMLR Sci.* **5:**259–271.

Goss, C., Middleton, D. and Rodhouse, P. (2001) Investigation of squid stocks using acoustic survey methods. *Fish. Res.* **54:**111–121.

Graham, J.B., Lowell, W.R., Chin Lai, N. and Laurs, R.M. (1989) O2 tension, swimming velocity, and thermal effects on the metabolic rate of the Pacific albacore, *Thunnus alalunga*. *Exp. Biol.* **48:**89–94.

Josse, E., Bach, P. and Lagorn, L. (1998) Simultaneous observations of tuna movements and their prey by sonic tracking and acoustic surveys. *Hydrobiologia* **371/372:** 61–69.

Kajiwara, Y., Iida, K. and Kamei, Y. (1990) Measurement of target strength for the flying squid *Ommastrephes bartrami*. *Bull. Fac. Fish., Hokkaido Univ.* **41:**205–212.

Laurs, R.M. (1983) The North Pacific albacore — an important visitor to California current waters. *CalCOFI Rep.* **14:**99–106.

Laurs, R.M. and Dotson, R.C. (1992) Albacore. In: *California's Living Marine Resources and Their Utilization*. W.S. Leet, C.M. Dewees & C.W. Haugen (eds) Sea Grant Extension Program, Davis, CA: Department of Wildlife and Fisheries Biology, University of California, Davis, pp. 136–138.

Laurs, R.M. and Lynn, R.J. (1977) Seasonal migration of North Pacific albacore, *Thunnus alalunga*, into North American coastal waters: distribution, relative abundance and association with transition zone waters. *Fish. Bull. US* **75:**795–822.

Laurs, R.M., Fiedler, P.C. and Montgomery, D.R. (1984) Albacore tuna catch distributions relative to environmental features observed from satellites. *Deep-Sea Res.* **31:**1085–1099.

Lukas, R. (2001) Pacific Ocean equatorial currents. In: *Encyclopedia of Ocean Sciences*. J.H. Steele, S.A. Thorpe & K.K. Turekian (eds). San Diego, CA: Academic Press, **4:**2069–2076.

MacLennan, D.N. and Simmonds, E.J. (1992) *Fisheries Acoustics*. New York: Chapman and Hall, pp. 323.

MacLennan, D.N., Fernandes, P.G. and Dalen, J. (2002) A consistent approach to definitions and symbols in fisheries acoustics. *ICES J. Mar. Sci.* **59:**365–369.

McGillicuddy, D.J., Robinson, A.R., Siegel, D.A. *et al.* (1998) Influence of mesoscale eddies on new production in the Sargasso Sea. *Nature* **394:**263–266.

McKelvey, D.R. (2000) *The use of two frequencies to interpret acoustic scattering layers*. MS Thesis, Seattle, WA: University of Washington.

Ménard, F., Lévénez, J.J., Potier, M., Ternon, J.F., Baurand, F., Maury, O. and Marsac, F. (2005) Acoustic characterization of tropical tuna prey in the Western Indian Ocean in relation with local environmental conditions. ICES C.M. 2005/U:11, pp. 13.

Mizuno, K., Okazaki, M. and Nakano, H. (1994) Analysis of catch depth by species for tuna longline fishery based on catch by branch lines. *Bull. Nat. Res. Inst. Far Seas Fish.* **34:**43–62.

Murphy, G.I. and Shomura, R.S. (1972) Pre-exploitation abundance of tunas in the equatorial central Pacific. *Fish. Bull. US* **70:**875–910.

Nakano, H.M., Okazaki, M. and Okamoto, H. (1997) Analysis of catch depth by species for tuna longline fishery based on catch by branch lines. *Bull. Nat. Res. Inst. Far Seas Fish.* **34:**43–62.

Oschlies, A. and Garcon, V. (1998) Eddy-induced enhancement of primary production in a model of the North Atlantic Ocean. *Nature* **394:**266–269.

Piontkovski, S.A., Williams, R. and Melnik, T.A. (1995) Spatial heterogeneity, biomass and size structure of plankton of the Indian Ocean: Some general trends. *Mar. Ecol. Prog. Ser.* **117:**219–227.

Qiu, B. and Chen, S. (2004) Seasonal modulations in the eddy field of the South Pacific Ocean. *J. Phys. Oceanogr.* **34:**1515–1527.

Ressler, P.H., Brodeur, R.D., Peterson, W.T. *et al.* (2004) The spatial distribution of euphausiid aggregations in the Northern California Current during August 2000. *Deep-Sea Res. II, Special Issue* **52:**89–108.

Saito, S. (1973) Studies on fishing of albacore, *Thunnus alalunga* (Bonnaterre), by experimental deep-sea tuna longline. *Mem. Fac. Fish., Hokkaido Univ.* **21:**107–184.

Sassa, C., Kawaguchi, K., Kinoshita, T. and Watanabe, C. (2002) Assemblages of vertical migratory mesopelagic fish in the transitional region of the western North Pacific. *Fish. Oceanogr.* **11:**193–204.

Seki, M.P., Polovina, J.J., Brainard, R.E., Bidigare, R.R., Leonard, C.L. and Foley, D.G. (2001) Biological enhancement at cyclonic eddies tracked with GOES thermal imagery in Hawaiian waters. *Geophys. Res. Lett.* **28:**1583–1586.

Seki, M.P., Lumpkin, R. and Flament, P. (2002) Hawaii cyclonic eddies and blue Marlin catches: the case study of the 1995 Hawaiian International Billfish Tournament. *J. Oceanogr.* **58:**739–745.

Swartzman, G. (2001) Spatial patterns of Pacific hake *Merluccius productus* shoals and euphausiid patches in the California Current System. In: *Spatial Processes and Management of Marine Populations: Proceedings of the Symposium on Spatial Processes and Management of Marine Populations, October 27–30, 1999, Anchorage, Alaska*. G.H. Kruse (ed.) Fairbanks, AK: Alaska Sea Grant College Program, pp. 495–512.

The Ring Group (1981) Gulf Stream cold-core rings: their physics, chemistry, and biology. *Science* **212:**1091–1100.

Wiebe, P.H. and Joyce, T.M. (1992) Introduction of interdisciplinary studies of Kuroshio and Gulf Stream rings. *Deep Sea Res. I.* **39:**v–vi.

Wiebe, P.H., Flierl, G.R., Davis, C.S., Barber, V. and Boyd, S.H. (1985) Macrozooplankton biomass in Gulf Stream warm-core rings: spatial distribution and temporal changes. *J. Geophys. Res.* **90:**8885–8901.

WPRFMC (2001) Pelagic fisheries of the Western Pacific region, 1999 Annual Report. Honolulu: Western Pacific Regional Fisheries Management Council.

Yamanaka, H. (1956) Vertical structure of the ocean and albacore fishing conditions in the vicinity of 10°S in the western South Pacific. *Bull. Jap. Soc. Fish.* **21:** 1187–1193.

Young, J.W., Lamb, T.D. and Bradfort, R.W. (1996) Distribution and community structure of midwater fishes in relation to the subtropical convergence off eastern Tasmania, Australia. *Mar. Biol.* **126:**571–584.

Zimmerman, R.A. and Briggs, D.C. (1999) Patterns of distribution of sound-scattering zooplankton in warm- and cold-core eddies in the Gulf of Mexico, from a narrowband acoustic Doppler current profiler survey. *J. Geophys. Res.* **104:**5251–5262.